



โครงการ

การเรียนการสอนเพื่อเสริมประสบการณ์

ชื่อโครงการ Interaction between Sweet Taste Receptor and Sweet-Tasting Proteins by using Molecular Dynamics Simulation

การจำลองแบบทางพลวัตเชิงโมเลกุลระหว่างตัวรับรสหวานในมนุษย์กับโปรตีนให้ความหวาน

ชื่อนิสิต นางสาวณัฐสร้อย หวังสว่างรุ่ง

ภาควิชา เคมี

ปีการศึกษา 2560

คณะวิทยาศาสตร์ จุฬาลงกรณ์มหาวิทยาลัย

Interaction between Sweet Taste Receptor and Sweet-Tasting
Proteins by using Molecular Dynamics Simulation

การจำลองแบบทางพลวัตเชิงโมเลกุลระหว่างตัวรับรสหวานในมนุษย์
กับโปรตีนให้ความหวาน

By

Miss Nutsarun Wangsawangrung

Submitted in partial fulfillment of the requirements for
the Bachelor of Science Program
Department of Chemistry, Faculty of Science
Chulalongkorn University
Academic Year 2017


Project Title Interaction between Sweet Taste Receptor and Sweet-Tasting Proteins by using
Molecular Dynamics Simulation


By Miss Nutsarun Wangsawangrung

Accepted by the Faculty of Science, Chulalongkorn University in Partial Fulfillment of the Requirements
for the Bachelor's Degree

Project Committee


..... Chairman
(Associate Professor Pakorn Varanusupakul, Ph.D.)


..... Project Advisor
(Professor Supot Hannongbua, Ph.D.)


..... Project Co-Advisor
(Assistant Professor Thanyada Rungrotmongkol, Ph.D.)


..... Examiner
(Associate Professor Preecha Phuwapraisirisan, Ph.D.)

This report has been endorsed by Head of Chemistry Department

..... Head of Chemistry Department
(Associate Professor Vudhichai Parasuk, Ph.D.)

Date..... Month..... Year.....

Overall Quality of this Report Excellent Satisfactory Somewhat Satisfactory

ชื่อโครงการ การจำลองแบบทางพลวัตเชิงโมเลกุลระหว่างตัวรับรสหวานในมนุษย์กับโปรตีนให้ความหวาน
 ชื่อนิสิตในโครงการ นางสาวณัฐสรีย์ หวังสว่างรุ่ง เลขประจำตัว 5733089423
 ชื่ออาจารย์ที่ปรึกษา ศาสตราจารย์ ดร.สุพจน์ ทารหนองบัว
 ชื่ออาจารย์ที่ปรึกษาร่วม ผู้ช่วยศาสตราจารย์ ดร.ธัญญดา รุ่งโรจน์มงคล
 ภาควิชาเคมี คณะวิทยาศาสตร์ จุฬาลงกรณ์มหาวิทยาลัย ปีการศึกษา 2560

บทคัดย่อ

ตัวรับรสหวานในมนุษย์ (hT1R2-hT1R3) ประกอบด้วยโปรตีน hT1R2 และ hT1R3 ซึ่งเป็นโปรตีนตัวรับแบบคู่จีตราสซี ในปัจจุบันนี้ยังไม่มีโครงสร้าง 3 มิติ ของตัวรับรสหวานในมนุษย์ จึงต้องใช้การจำลองโครงสร้าง 3 มิติ ด้วยเทคนิคโฮโมโลยีโมเดลลิง ตัวรับรสหวานในมนุษย์สามารถยึดจับกับสารเคมีได้หลายชนิดไม่ว่าจะเป็นน้ำตาลที่พบได้ในธรรมชาติ กรดอะมิโน รวมไปถึงน้ำตาลเทียมหรือน้ำตาลสังเคราะห์ นอกจากนั้นยังสามารถยึดจับกับโปรตีนให้ความหวาน เช่น บลาซซีน ได้อีกด้วย แต่อย่างไรก็ตามยังไม่มียานวิจัยที่เกี่ยวข้องกับการยึดจับกันระหว่างตัวรับรสหวานในมนุษย์กับโปรตีนให้ความหวานมากนัก ดังนั้นในงานวิจัยนี้จึงมุ่งศึกษาและเปรียบเทียบการยึดจับของบลาซซีนกับตัวรับรสหวานในมนุษย์ทั้ง 2 โครงสร้าง คือ closed-hT1R2/open-hT1R3 และ open-hT1R2/closed-hT1R3 ด้วยการจำลองแบบทางพลวัตเชิงโมเลกุล และการศึกษาอันตรกิริยาระหว่างโปรตีน พบว่าบลาซซีนยึดจับกับโครงสร้างที่เป็น open form ของ closed-hT1R2/open-hT1R3 ได้ดีกว่า open-hT1R2/closed-hT1R3 ซึ่งผลการวิจัยนี้ทำให้เข้าใจเกี่ยวกับอันตรกิริยาระหว่างตัวรับรสหวานในมนุษย์และโปรตีนให้ความหวานมากยิ่งขึ้น

คำสำคัญ: ตัวรับรสหวานในมนุษย์, hT1R2-hT1R3, โปรตีนให้ความหวาน, บลาซซีน, การจำลองแบบทางพลวัตเชิงโมเลกุล

Project Title Interaction between Sweet Taste Receptor and Sweet-Tasting Proteins by using
Molecular Dynamics Simulation

Student Name Miss Nutsarun Wangsawangrung Student ID 5733089423

Advisor Name Professor Supot Hannongbua, Ph.D.

Co-advisor Name Assistant Professor Thanyada Rungrotmongkol, Ph.D.

Department of Chemistry, Faculty of Science, Chulalongkorn University, Academic Year 2017

Abstract

The human sweet taste receptor (hT1R2-hT1R3) is the heteromeric complex composed of hT1R2 and hT1R3 subunits belonging to the class C G-protein-coupled receptors (GPCRs). The crystal structure of hT1R2-hT1R3 is not available in nowadays, so homology modeling was applied to model the hT1R2-hT1R3. The hT1R2-hT1R3 can bind with a wide variety of chemical substances including naturally occurring sugars, D-amino acids, as well as artificial chemical compounds. Moreover, naturally sweet-taste proteins, such as brazzein also bind to hT1R2-hT1R3 but the interaction remains unclear. In this study, brazzein was docking to the 2 forms of hT1R2-hT1R3, which are closed-hT1R2/open-hT1R3 and open-hT1R2/closed-hT1R3. The molecular dynamics simulation and intermolecular interactions between proteins suggested that brazzein preferred to bind with the open form subunit of closed-hT1R2/open-hT1R3 rather than open-hT1R2/closed-hT1R3. These results could provide a more understanding of interaction between human sweet taste receptor and brazzein.

Keywords: Human sweet taste receptor, hT1R2-hT1R3, sweet-taste proteins, Brazzein, Molecular dynamics simulation

Acknowledgement

I am very grateful to my advisor, Professor Supot Hannongbua, PhD. and my co-advisor, Assistant Professor Thanyada Rungrotmongkol, Ph.D. who always give a helpful suggestion and advices along the project. I also thank to Ms. Wanwisa Panman (P'May) who always support with every information and hand-on practice in computational study.

Finally, I would like to thank my family and friends who always give me the power to work with this project.



Contents

	Page
บทคัดย่อ	iii
Abstract	iv
Acknowledgements	v
Contents	vi
List of Figures	viii
List of Tables	x
Abbreviation Index	xi
Chapter 1 Introduction	1
1.1 Background and motivation of study	1
1.2 Objectives of the study	1
1.3 Benefits of the study	2
1.4 Related studies	2
1.5 A tongue of human	2
1.6 A sweet taste receptor	4
1.7 A Sweet-taste protein	5
1.8 Homology modeling	5
1.9 Molecular docking simulation	6
1.10 Molecular dynamics simulation	7
1.11 Binding free energy calculations	8
Chapter 2 Methods	9
2.1 Materials	9
2.2 Preparation of 3D structure of human sweet taste receptor	10
2.3 Preparation of 3D structure of brazzein	12
2.4 Molecular docking simulation	13
2.5 System preparations	14
2.6 Molecular Dynamics Simulation	14
2.7 Binding Free Energy Calculations	15

Chapter 3 Results and Discussion	16
3.1 Homology modeling of human sweet taste receptor	16
3.2 Molecular docking simulation	20
3.3 Molecular dynamics simulation	21
3.4 System stability	22
3.5 Structural stability	25
3.6 Binding affinity prediction	26
3.7 Contact residues for brazzein binding	27
3.8 Hydrogen bonding interaction	30
Chapter 4 Conclusion	32
References	33
Curriculum Vitae	35



List of Figures

	Page
Figure 1.1 Tongue of human.	3
Figure 1.2 Taste bud.	3
Figure 1.3 Sweet taste receptor T1R2-T1R3.	4
Figure 1.4 3D structure of Brazzein.	5
Figure 1.5 Molecular docking between target and ligand.	6
Figure 2.1 The crystal structure of mGluR1 as template protein for constructing the hT1R2-hT1R3 modelled structures.	10
Figure 2.2 GenBank website.	11
Figure 2.3 ORF Finder website.	11
Figure 2.4 Swiss Model website.	12
Figure 2.5 The solution NMR structure of sweet protein brazzein.	12
Figure 2.6 ClusPro server.	13
Figure 2.7 PROPKA website.	14
Figure 3.1 Sequence alignment between mGluR1 (closed-mT1R2) and hT1R2.	16
Figure 3.2 Sequence alignment between mGluR1 (closed-mT1R2) and hT1R3.	17
Figure 3.3 Sequence alignment between mGluR1 (open-mT1R3) and hT1R2.	17
Figure 3.4 Sequence alignment between mGluR1 (open-mT1R3) and hT1R3.	18
Figure 3.5 The models of human sweet taste receptor: (a) closed-hT1R2/open-hT1R3 and (b) open-hT1R2/closed-hT1R3.	18
Figure 3.6 Superimposition between mGluR1 template and the models of human sweet taste receptor: (a) closed-hT1R2/open-hT1R3 and (b) open-hT1R2/closed-hT1R3.	19
Figure 3.7 Homology models of human sweet taste receptor: (a) closed-hT1R2/open-hT1R3 and (b) open-hT1R2/closed-hT1R3.	19
Figure 3.8 Two possible structures of closed-hT1R2/open-hT1R3 in complex with brazzein: (a) complex 1 and (b) complex 2.	20
Figure 3.9 Three possible structures of open-hT1R2/closed-hT1R3 with brazzein: (a) complex 1, (b) complex 2 and (c) complex 3.	21
Figure 3.10 Last snapshot of closed-hT1R2/open-hT1R3 with Brazzein: (a) complex 1 and (b) complex 2.	22


- Figure 3.11** Last snapshot of open-hT1R2/closed-hT1R3 with Brazzein: (a) complex 1, (b) complex 2 and (c) complex 3. 22
- Figure 3.12** RMSD plots of all atoms for systems: (a) closed-hT1R2/open-hT1R3 receptor in apo form and (b-c) in brazzein bound forms, (d) open-hT1R2/closed-hT1R3 receptor in apo form and (e-g) in brazzein bound forms. 23
- Figure 3.13** 2D-RMSD plots of hT1R2, hT1R3 and brazzein for closed-hT1R2/open-hT1R3 and open-hT1R2/closed-hT1R3 in apo and brazzein bound forms. 24
- Figure 3.14** B-factor and RMSF values of all atoms for systems: (a) closed-hT1R2/open-hT1R3 receptor in apo form and (b-c) in brazzein bound forms, (d) open-hT1R2/closed-hT1R3 receptor in apo form and (e-g) in brazzein bound forms. 25
- Figure 3.15** Per-residue decomposition free energy ($\Delta G_{\text{bind}}^{\text{residue}}$, kcal/mol) of hT1R2 (left) and hT1R3 (right) domains for brazzein binding with closed-hT1R2/open-hT1R3 (a-d) and open-hT1R2/closed-hT1R3 (e-j) based on MM/GBSA method. 28
- Figure 3.16** The decomposition free energy (kcal/mol) from the residue (blue bar), side chain (red bar) and backbone (green bar) of closed-hT1R2/open-hT1R3 receptor contributing to brazzein binding. The electrostatic ($\Delta E_{\text{ele}} + \Delta G_{\text{psolv}}$) and vdW ($\Delta E_{\text{vdW}} + \Delta G_{\text{nsolv}}$) energetic terms were represented by black and light grey lines, respectively. 29
- Figure 3.17** The decomposition free energy (kcal/mol) from the residue (blue bar), side chain (red bar) and backbone (green bar) of open-hT1R2/closed-hT1R3 receptor contributing to brazzein binding. The electrostatic ($\Delta E_{\text{ele}} + \Delta G_{\text{psolv}}$) and vdW ($\Delta E_{\text{vdW}} + \Delta G_{\text{nsolv}}$) energetic terms were represented by black and light grey lines, respectively. 29
- Figure 3.18** The number of H-bond between hT1R2 and brazzein, hT1R3 and brazzein for brazzein binding with closed-hT1R2/open-hT1R3 (a-b) and open-hT1R2/closed-hT1R3 (c-e). 30
- Figure 3.19** The number of H-bond between hT1R2 and hT1R3 for (a) closed-hT1R2/open-hT1R3 in apo form, (b-c) brazzein binding with closed-hT1R2/open-hT1R3, (d) open-hT1R2/closed-hT1R3 in apo form and (e-f) brazzein binding with open-hT1R2/closed-hT1R3. 31

List of Table

	Page
Table 3.1 The interaction energies (kcal/mol) between closed-hT1R2/open-hT1R3 and brazzein.	20
Table 3.2 The interaction energies (kcal/mol) between open-hT1R2/closed-hT1R3 and brazzein.	21
Table 3.3 The binding free energy (kcal/mol) of the complexes between closed-hT1R2/open-hT1R3, open-hT1R2/closed-hT1R3 bind with brazzein.	26



Abbreviation Index



T1R2	taste receptor type 1 subtypes 2
T1R3	taste receptor type 1 subtypes 3
hT1R2-hT1R3	human sweet taste receptor
TRCs	taste receptor cells
mGluR1	metabotropic glutamate receptor subtypes 1
GPCRs	G Protein Coupled Receptors
ATD	Amino Terminal Domain
VFT	Venus Flytrap Domain
CRD	Cysteine-Rich Domain
PDB	Protein Data Bank
MD	Molecular Dynamics
RMSD	Root-Mean-Square Deviation
RMSF	Root-Mean-Square Fluctuation
MM/GBSA	Molecular Mechanics/Generalized Born Surface Area
AMBER	Assisted Model Building with Energy Refinement
SD	Steepest Descents
CG	Conjugated Gradient
PME	Particle Mesh Ewald

Chapter 1

Introduction

1.1 Background and motivation of study

Nowadays, the number of patients suffering from diseases caused by the consumption of sugar has become a global health problem. Artificial low calorie sweeteners have been used instead of sucrose to sweeten foods and beverages, because they have low calories and sweeter than sucrose. However, if one consumes for a long term, it may have severe side effects such as mental health problems, emotional disorders, brain tumor etc.

The sweet-taste proteins are being interested in how they bind with human sweet taste receptor, because they come from natural, do not cause tumor and are more than 1000 times sweeter than sucrose. One of the sweet-taste proteins is brazzein. It is 2,000 times sweeter than sucrose. Brazzein comes from a climbing berry plant that grows in West African countries such as Angola, Gabon, Congo, and Nigeria.

Human can detect all 5 tastes: sweet, bitter, sour, salty and umami through different protein receptors. Sweet taste receptor is taste receptor type 1 subtypes 2 and 3 (T1R2, T1R3). So, sweet taste receptor of human (hT1R2-hT1R3) is a heterodimer of T1R2 and T1R3. Up to date, hT1R2-hT1R3 has no crystal structure and thus homology modeling is used to predict the 3D structure of this complex.

In this research project, we studied how brazzein binds with hT1R2-hT1R3 using computational techniques including molecular docking and molecular dynamics simulation. The binding free energies of hT1R2-hT1R3 with brazzein bound at different sites were investigated and compared. We also identified the critical residues that important for brazzein binding. These results lead us a more understanding about the interactions between hT1R2-hT1R3 and brazzein.

1.2 Objectives of the study

1.2.1 To study and compare the efficiency of brazzein binding to the hT1R2-hT1R3 heterodimer.

1.2.2 To identify the key residues important for brazzein binding.

1.3 Benefits of the study

1.3.1 Better understanding on the molecular recognition of hT1R2-hT1R3 toward brazzein.

1.3.2 3D structure of complex between hT1R2-hT1R3 and brazzein and amino acid residues in the interface area.

1.4 Related studies

In 2006, Eric Walters and Goran Hellekant [1] studied about interaction of the sweet protein brazzein with the 2 forms of sweet taste receptor hT1R2-hT1R3 by Molecular docking simulation. The sequences of the human T1R2 and T1R3 ligand binding domains were used to conduct a FASTA search (the tool provides sequence similarity searching against protein databases.) [2] of the sequences in the RCSB Protein Data Bank (the website that contains information about the 3D structures of proteins, nucleic acids, and complex assemblies.) [3]. They identified the most appropriate structure of the ligand binding domain of the metabotropic glutamate receptor mGluR1 with 2 bound glutamate molecules, one subunit in open conformation and another subunit in closed conformation, 1EWK. There are 2 possibilities conformations: closed-T1R2/open-T1R3 and open-T1R2/closed-T1R3. They used this structure, 1EWK, as template for homology modeling and alignment the T1R sequences in the Pfam database [4] by using Molecular Operating Environment (MOE) Homology Model module. The GRAMM docking consistently places brazzein into the binding site of the open subunit.

1.5 A tongue of human

The human tongue (Figure 1.1) can detect 5 basic tastes including sweet, sour, salty, bitter and umami. The chemical substance responsible for the taste is released in the mouth and comes into contact with a nerve cell. It activates the cell by changing specific proteins in the wall of the sensory cell. This change causes the sensory cell to transmit messenger substances, which in turn activate further nerve cells. These nerve cells then pass information for a particular perception of flavor on to the brain. The numerous wart-like bumps on the mucous membrane of the tongue are where the substance producing the taste is transformed into a nerve signal. These bumps, which are called taste papillae, contain many sensory cells with a special structure. There are three types categorized by their shapes: fungiform papillae, circumvallate papillae and foliate papillae [5].

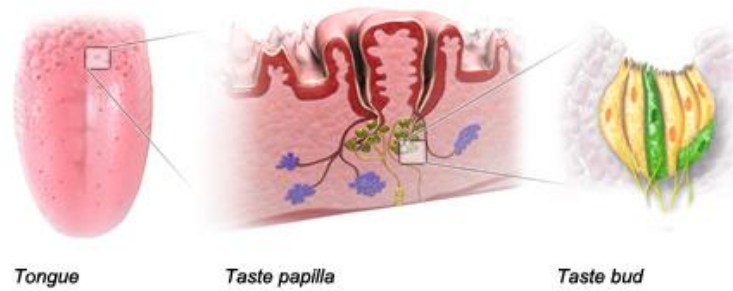


Figure 1.1 Tongue of human [5].

The taste buds (Figure 1.2) are located in the walls and grooves of the papillae. They have numerous sensory cells that are in turn connected to many different nerve fibers. Each taste bud has between 10 and 50 sensory cells. These cells form a capsule that is shaped like a flower bud or an orange. At the tip of this capsule, there is a pore that works as a fluid-filled funnel. This funnel contains thin, finger-shaped sensory cell extensions, which are called taste hairs. Proteins on the surface bind chemicals to the cell for tasting [5].

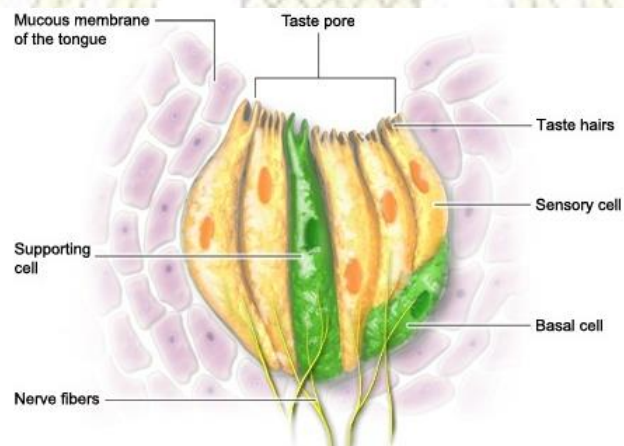


Figure 1.2 Taste bud [5].

1.6 A sweet taste receptor

Taste processing is first achieved at the level of taste receptor cells (TRCs) which are clustered in taste buds on the tongue. When TRCs are activated by specific tastants, they transmit information via sensory afferent fibers to specific areas in the brain that are involved in taste perception. Four morphologic subtypes of TRCs have been identified. Type I glial-like cells detect salty taste. Type II cells express G-protein coupled receptors (GPCRs) to detect sweet, umami, and bitter tastes. Type III cells sense sour stimuli, while Type IV cells likely represent stem or progenitor taste cells [6].

The sweet taste receptor is composed of two distinct G protein-coupled receptors (GPCRs): type 1, member 2 (T1R2) and type 1, member 3 (T1R3). The T1R2/T1R3 sweet taste receptor responds to various chemically distinct compounds, such as natural sugars, noncaloric artificial and natural sweeteners, some D-amino acids, and sweet-tasting proteins [7].

The T1R2 and T1R3 subunits (Figure 1.3) are members of the small family of class C GPCRs. Class C GPCRs share a common architecture, including a large amino terminal domain (ATD). This ATD contains a Venus flytrap domain (VFT) and a short cysteine-rich domain (CRD), which connects the ATD to the α -helical transmembrane domain characteristic of GPCRs [8].

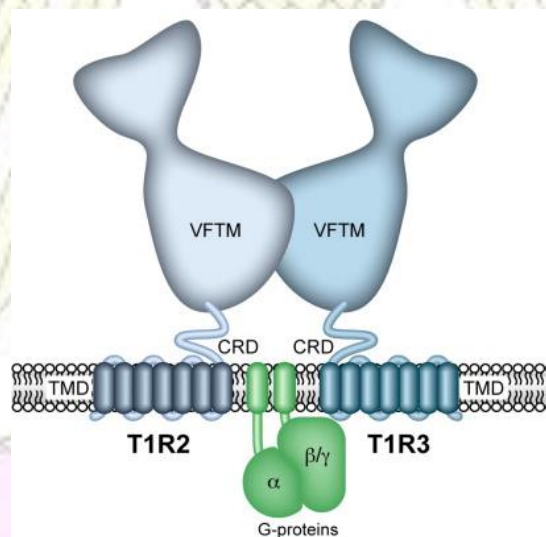


Figure 1.3 Sweet taste receptor T1R2-T1R3 [9].

1.7 A Sweet-taste protein

Brazzein is the smallest sweet-taste protein that contains 54 amino acids (Figure 1.4). Brazzein is found in African plant *Pentadiplandra brazzeana* and is very stable over a wide range of temperatures and various pH levels [10]. It has sweet taste 2,000 times sweeter than sucrose for equal weights and represents an excellent alternative to available low calorie sweeteners [11].

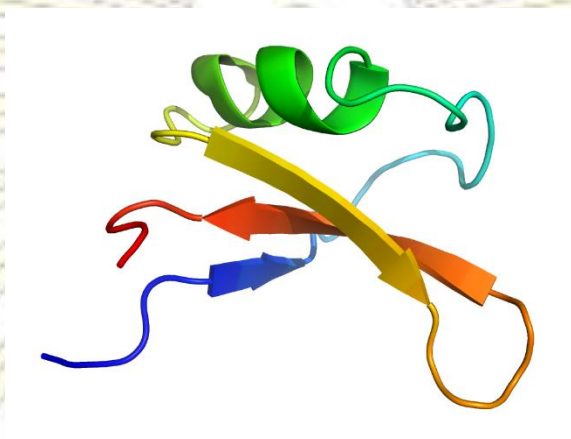


Figure 1.4 3D structure of Brazzein [12].

1.8 Homology modeling

Protein structure determination using experimental methods such as X-ray crystallography or NMR spectroscopy is not successful with all proteins [13]. Computational methods could possibly solve this problem by prediction the structure of proteins. Homology modeling has become a popular tool to build 3D structures of molecular targets, which experimental structures are not available in databases [14]. The 3D structure of a protein sequence based primarily on its sequence similarity to one or more proteins of known structures [15].

Given a protein sequence, homology modeling usually consists of the following four steps [16]:

- 1) Identify the homologue of known structure from the Protein Data Bank.
- 2) Align the query sequence to the template structure.
- 3) Build the model based on the alignment.
- 4) Assess and refine the model.

1.9 Molecular docking simulation

Molecular docking (Figure 1.5) is the technique that give a prediction of the ligand-protein and protein-protein complex structures. Docking can be achieved through two interrelated steps: first by sampling conformations of the ligand or protein in the active site or binding site of the protein; then ranking these conformations via a scoring function. Ideally, sampling algorithms should be able to reproduce the experimental binding mode and the scoring function should also rank it highest among all generated conformations [17]. The early elucidation for the ligand-receptor binding mechanism is the lock-and-key theory proposed by Fischer [18], in which the ligand fits into the receptor like lock and key.



Figure 1.5 Molecular docking between target and ligand [19].

The ClusPro server is a server that widely used for protein–protein docking. This server performs three computational steps as follows [20]:

- 1) Rigid-body docking by sampling billions of conformations uses PIPER [21], a docking program.
- 2) Root-Mean-Square Deviation (RMSD)-based clustering of the 1,000 lowest-energy structures generated, to find the largest clusters that will represent the most likely models of the complex.
- 3) Refinement of selected structures using energy minimization

PIPER represents the interaction energy between two proteins using an expression of the form:

$$E = 0.40E_{\text{rep}} + (-0.40)E_{\text{att}} + 600E_{\text{elec}} + 1.00E_{\text{DARS}}$$

Where E_{rep} = the repulsive contributions to the van der Waals interaction energy
 E_{att} = the attractive contributions to the van der Waals interaction energy
 E_{elec} = an electrostatic energy term
 E_{DARS} = a pairwise structure-based potential constructed by the 'decoys as the reference state' (DARS) [22] approach.

1.10 Molecular dynamics simulation

Molecular dynamics (MD) simulation is computational method, which calculates the time-dependent behavior of a molecular system. MD simulations have provided detailed information on the fluctuations and conformational changes of proteins and nucleic acids. These methods are now routinely used to investigate the structure, dynamics and thermodynamics of biological molecules and their complexes. The molecular dynamics simulation method is based on Newton's second law or the equation of motion. It is possible to determine the acceleration of each atom in the system. Integration of the equations of motion then yields a trajectory that describes the positions, velocities and accelerations of the particles as they vary with time [23].

$$F_i = m_i a_i = m_i \frac{d^2 r_i}{dt^2}$$

Where F_i = the force exerted on particle i
 m_i = the mass of particle i
 a_i = the acceleration of particle i
 r_i = the position vector of particle i (x_i, y_i, z_i)
 t = time

Potential energies are calculated by molecular mechanics force fields. The molecular systems are minimized and prepared parameters for MD simulations using AMBER 16 program.

Thermodynamic properties of the system are canonical ensemble (NVT), isothermal-isobaric (NPT) ensemble, and generalized ensembles that used to control the system. When the system is stable, data can be used for analysis.

1.11 Binding free energy calculations

The binding free energy (ΔG_{bind}) of the protein-ligand complexes was calculated using MM/PBSA and MM/GBSA approaches [24]. Herein, the ΔG_{bind} is estimated from the free energy difference between protein-ligand complex and the individual forms,

$$\Delta G_{\text{bind}} = G_{\text{complex}} - (G_{\text{protein}} + G_{\text{ligand}})$$

The ΔG_{bind} composes of the molecular mechanics energy (ΔE_{MM}), solvation free energy (ΔG_{solv}), and entropic term ($T\Delta S$) as represented

$$\Delta G_{\text{bind}} = \Delta E_{\text{MM}} + \Delta G_{\text{solv}} - T\Delta S$$

Where

ΔG_{bind}	=	binding free energy
ΔE_{MM}	=	molecular mechanical energy
ΔG_{solv}	=	solvation free energy
T	=	temperature
ΔS	=	entropy

The ΔE_{MM} contains bonded and non-bonded energies, comprising the electrostatic (ΔE_{ele}) and van der Waals energies (ΔE_{vdW}), whereas the ΔG_{solv} consists of polar and nonpolar terms,

$$\Delta G_{\text{solv}} = \Delta G_{\text{solv}}^{\text{ele}} + \Delta G_{\text{solv}}^{\text{nonpolar}}$$

The $\Delta G_{\text{solv}}^{\text{ele}}$ is estimated using either the Poisson-Boltzmann (PB) or the generalized Born (GB) equations, whereas the $\Delta G_{\text{solv}}^{\text{nonpolar}}$ is calculated using solvent accessible surface area (SASA) [25].

Chapter 2

Methods

2.1 Materials

- 2.1.1 High-performance computing
- 2.1.2 Ubuntu operating system version 14.04
- 2.1.3 Programs and websites
 - 2.1.3.1 Protein Data Bank (PDB)
 - 2.1.3.2 GenBank
 - 2.1.3.3 ORF Finder
 - 2.1.3.4 Swiss Model
 - 2.1.3.5 PROPKA
 - 2.1.3.6 GaussView 5.0
 - 2.1.3.7 Discovery Studio 3.0
 - 2.1.3.8 ClusPro
 - 2.1.3.9 SSH Secure Shell
 - 2.1.3.10 AMBER 16
 - 2.1.3.11 EditPlus
 - 2.1.3.12 OriginPro 8
 - 2.1.3.13 OriginPro 9.0
 - 2.1.3.14 Chimera 1.11.2
 - 2.1.3.15 VMD 1.9.2
 - 2.1.3.16 VideoMach

2.2 Preparation of 3D structure of human sweet taste receptor

The 3D structure of human sweet taste receptor (hT1R2-hT1R3) was built using the crystal structure of mGluR1 solved in active form (glutamate-bound with protein data bank code 1EWK) as the template protein (Figure 2.1) for homology models. The nucleotide sequences of hT1R2 and hT1R3 were obtained from GenBank website (Figure 2.2) codes BK000151 and BK000152, respectively. ORF Finder website (Figure 2.3) were used to change nucleotide sequences to protein sequences. Homology models of hT1R2-hT1R3 closed and open form have been constructed with the Swiss Model website (Figure 2.4). Building the closed conformation models of hT1R2 and hT1R3, closed-mT1R2 of mGluR1 was used as the template and the target sequences were hT1R2 and hT1R3 protein sequences, while open-mT1R3 of mGluR1 was used as the template for build the open conformation of hT1R2 and hT1R3.

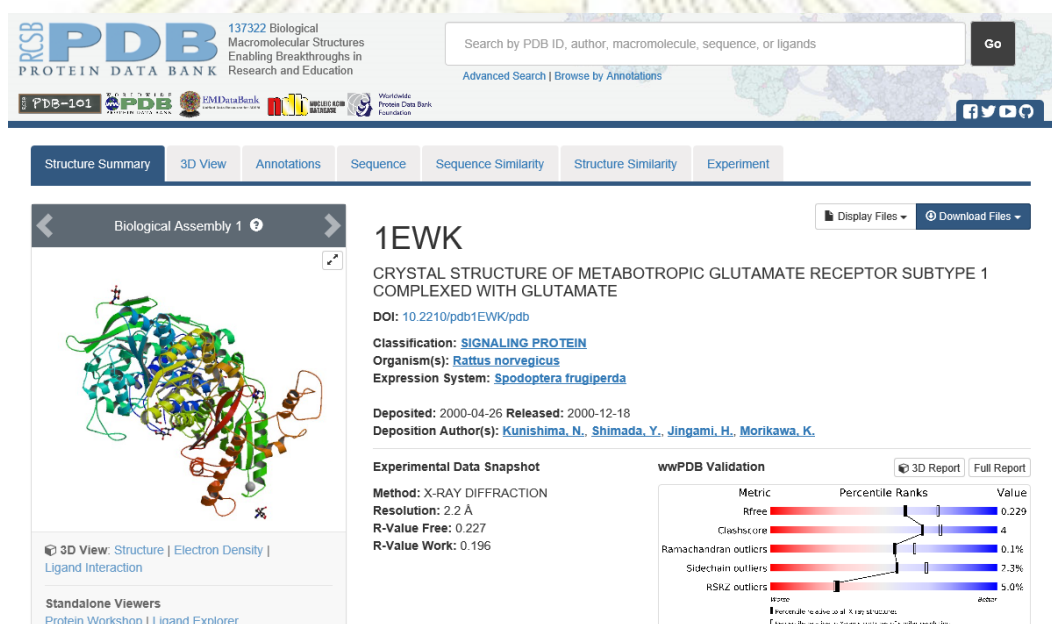


Figure 2.1 The crystal structure of mGluR1 as template protein for constructing the hT1R2-hT1R3 modelled structures.

GenBank

GenBank ▾ Submit ▾ Genomes ▾ WGS ▾ Metagenomes ▾ TPA ▾ TSA ▾ INSDC ▾ Other ▾

GenBank Overview

What is GenBank?

GenBank[®] is the NIH genetic sequence database, an annotated collection of all publicly available DNA sequences ([Nucleic Acids Research, 2013 Jan;41\(D1\):D36-42](#)). GenBank is part of the [International Nucleotide Sequence Database Collaboration](#), which comprises the DNA DataBank of Japan (DDBJ), the European Nucleotide Archive (ENA), and GenBank at NCBI. These three organizations exchange data on a daily basis.

A GenBank release occurs every two months and is available from the [ftp site](#). The [release notes](#) for the current version of GenBank provide detailed information about the release and notifications of upcoming changes to GenBank. Release notes for [previous GenBank releases](#) are also available. GenBank growth statistics for both the traditional GenBank divisions and the WGS division are available from each release. GenBank growth [statistics](#) for both the traditional GenBank divisions and the WGS division are available from each release.

An [annotated sample GenBank record](#) for a *Saccharomyces cerevisiae* gene demonstrates many of the features of the GenBank flat file format.

Access to GenBank

There are several ways to search and retrieve data from GenBank.

- Search GenBank for sequence identifiers and annotations with [Entrez Nucleotide](#), which is divided into three divisions: [CoreNucleotide](#) (the main collection), [dbEST](#) (Expressed Sequence Tags), and [dbGSS](#) (Genome Survey Sequences).
- Search and align GenBank sequences to a query sequence using [BLAST](#) (Basic Local Alignment Search Tool). BLAST searches CoreNucleotide, dbEST, and dbGSS independently; see [BLAST info](#) for more information about the numerous BLAST databases.
- Search, link, and download sequences programatically using [NCBI e-utilities](#).
- The ASN.1 and flatfile formats are available at NCBI's anonymous FTP server: <ftp://ftp.ncbi.nlm.nih.gov/ncbi-asn1> and <ftp://ftp.ncbi.nlm.nih.gov/genbank>.

GenBank Resources

- [GenBank Home](#)
- [Submission Types](#)
- [Submission Tools](#)
- [Search GenBank](#)
- [Update GenBank Records](#)

Figure 2.2 GenBank website.

ORFfinder

Open Reading Frame Finder

ORF finder searches for open reading frames (ORFs) in the DNA sequence you enter. The program returns the range of each ORF, along with its protein translation. Use ORF finder to search newly sequenced DNA for potential protein encoding segments, verify predicted protein using newly developed SMART BLAST or regular BLAST.

This web version of the ORF finder is limited to the subrange of the query sequence up to 50 kb long. Stand-alone version, which doesn't have query sequence length limitation, is available for [Linux x64](#).

Examples (click to set values, then click Submit button):

- NC_011604 *Salmonella enterica* plasmid pWES-1, genetic code: 11; 'ATG' and alternative initiation codons; minimal ORF length: 300 nt
- NM_000059, genetic code: 1; start codon: 'ATG only'; minimal ORF length: 150 nt

Enter Query Sequence

Enter accession number, gi, or nucleotide sequence in FASTA format:

From: To:




Figure 2.3 ORF Finder website.

The screenshot shows the 'Start a New Modelling Project' interface on the SWISS-MODEL website. At the top, there is a navigation bar with 'Modelling', 'Repository', 'Tools', 'Documentation', 'Log in', and 'Create Account'. The main form area includes a 'Target Sequence(s)' field with a 'Paste your target sequence(s) or UniProtKB AC here' placeholder, an 'Upload Target Sequence File...' button, and a 'Validate' button. Below this is a 'Template File' section with an 'Add Template File...' button. The 'Project Title' field is set to 'Untitled Project' and the 'Email' field is 'Optional'. A 'Build Model' button is at the bottom. On the right, a 'Supported Inputs' dropdown menu is open, showing options: 'Sequence(s)', 'Target-Template Alignment', 'User Template', and 'DeepView Project'. A small disclaimer at the bottom of the form reads: 'By using the SWISS-MODEL server, you agree to comply with the following terms of use and to cite the corresponding articles.'

Figure 2.4 Swiss Model website.

2.3 Preparation of 3D structure of brazzein

The 3D structure of sweet protein brazzein was obtained from protein data bank code 2BRZ (Figure 2.5).

The screenshot displays the PDB website page for entry 2BRZ. The header includes the PDB logo, the text '137322 Biological Macromolecular Structures Enabling Breakthroughs in Research and Education', and a search bar. Below the header, there are navigation tabs: 'Structure Summary', '3D View', 'Annotations', 'Sequence', 'Sequence Similarity', 'Structure Similarity', and 'Experiment'. The '3D View' tab is active, showing a 3D ribbon diagram of the protein structure. To the right of the structure, the entry title is '2BRZ SOLUTION NMR STRUCTURE OF THE SWEET PROTEIN BRAZZEIN, MINIMIZED AVERAGE STRUCTURE'. Below the title, it lists the DOI (10.2210/pdb2BRZ/pdb), classification as 'SWEET PROTEIN', and organism as 'Pentadiplandra brazzeana'. It also provides deposition and release dates (1998-04-30 and 1998-07-01) and the deposition author(s): Caldwell, J.E., Abildgaard, F., Dzakula, Z., Ming, D., Hellekant, G., Markley, J.L. A 'wwPDB Validation' section is present, showing a table of metrics and percentile ranks.

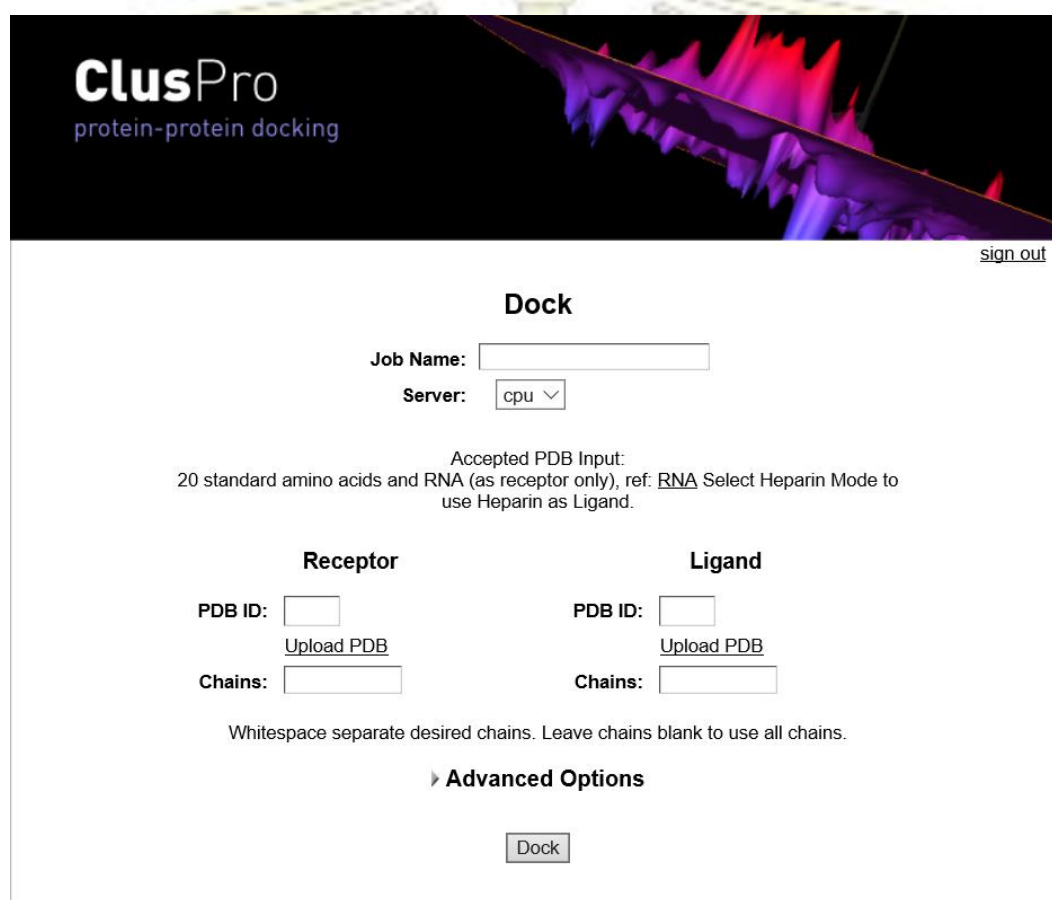
Metric	Percentile Ranks	Value
Clashscore	27	27
Ramachandran outliers	23.1%	23.1%
Sidechain outliers	40.0%	40.0%

Legend for wwPDB Validation:
 ■ Percentile relative to all structures.
 ■ Percentile relative to all NMR structures.

Figure 2.5 The solution NMR structure of sweet protein brazzein.

2.4 Molecular docking simulation

Protein-protein docking server, ClusPro (Figure 2.6), was used for the docking study. Brazzein was blind docked into the receptor closed-hT1R2/open-hT1R3 and open-hT1R2/closed-hT1R3. About 30 poses of docking simulation were shown for each of the receptor. The brazzein binding with the receptor with the low interaction energy of complex structure is used as criteria to choose the possible complexes for molecular dynamics simulation. The protonation state of all ionization residues of complexes were characterized by PROPKA website (Figure 2.7).



The image shows the ClusPro protein-protein docking server interface. At the top left, the logo reads "ClusPro protein-protein docking". On the top right, there is a "sign out" link. The main heading is "Dock". Below this, there is a "Job Name:" text input field and a "Server:" dropdown menu currently set to "cpu". A note states: "Accepted PDB Input: 20 standard amino acids and RNA (as receptor only), ref: RNA Select Heparin Mode to use Heparin as Ligand." The interface is divided into two columns: "Receptor" and "Ligand". Each column has a "PDB ID:" text input field with an "Upload PDB" link below it, and a "Chains:" text input field. A note below these fields says: "Whitespace separate desired chains. Leave chains blank to use all chains." At the bottom, there is a section for "Advanced Options" and a "Dock" button.

Figure 2.6 ClusPro server.

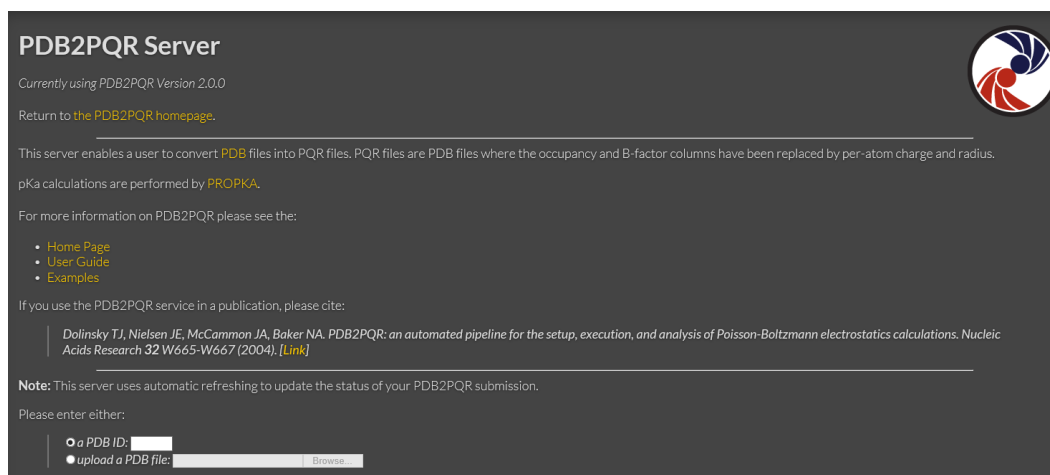


Figure 2.7 PROPKA website.

2.5 System preparations

All system preparations were performed by using AMBER16 program. The missing hydrogen atoms were added using the tLEaP module in AMBER. The AMBER ff14SB force field was applied for proteins. Each complex was solvated in the 12 Å octrahedral box of TIP3P water and Na⁺ ions were added to neutralize the system. Prior to performing MD simulation, the hydrogen atoms and water molecules were minimized with 3,000 steps of steepest descents (SD) and conjugated gradient (CG), while all protein atoms were restrained. After that, each system was minimized all atom with 1000 step of SD and 1500 step of CG.

2.6 Molecular Dynamics Simulation

MD simulation was performed under periodic boundary condition. All covalent bonds involving hydrogen atom were fixed by SHAKE algorithm. The short-range cutoff of 10 Å was employed for non-bonded interactions, while the Particle Mesh Ewald (PME) summation method was applied for calculating the long-range electrostatic interactions. Langevin algorithm has been applied to control temperature with a collision frequency of 0.002 ps for the 1 ns. The system was heated up from 100.0 to 310.0 K for 0.002 ps. Afterwards, the simulation was implemented with NPT ensemble at this temperature and pressure of 1 atm using the PMEMD module in AMBER16. Each system was simulated until the simulation time reached 100 ns and the snapshots were collected 5,000 in every 1 ns along the simulation.

2.7 Binding Free Energy Calculations

The binding free energy (ΔG_{bind}) of the complexes was calculated by using MM/GBSA approaches over the 100 trajectories taken from the last 20 ns by MM/GBSA.py program in AMBER16. Moreover, the energy composition was calculated to support the binding affinity by using MM/GBSA approach, and the protein/protein interactions in term of hydrogen bonding were also measured.



Chapter 3

Results and Discussion

3.1 Homology modeling of human sweet taste receptor

SWISS-MODEL, the web server, was used to create the homology models of human sweet taste receptor (Figures 3.1-3.4) by using the crystal structure of mGluR1 (closed-mT1R2 and open-mT1R3) code 1EWK as the template and using hT1R2 and hT1R3 protein sequences from GenBank (codes BK000151 and BK000152, respectively) as the target sequence. Closed-hT1R2 and closed-hT1R3 have sequence identity (and similarity) with its template, closed-mT1R2 of mGluR1, of 24.34% (39.75%) and 22.35% (39.09%), respectively, while open-hT1R2 and open-hT1R3 have sequence identity (and similarity) with its template, open-mT1R3 of mGluR1, of 24.47% (39.88%) and 22.01% (40.37%), respectively. The models of human sweet taste receptor closed-hT1R2/open-hT1R3 and open-hT1R2/closed-hT1R3 were shown in Figures 3.5a and 3.5b, respectively. The superimposition between the mGluR1 template and the models of human sweet taste receptor using Discovery Studio 2.5 were depicted in Figures 3.6a and 3.6b, respectively. Finally, the homology models of closed-hT1R2/open-hT1R3 (Figure 3.7a) and open-hT1R2/closed-hT1R3 were obtained as shown in Figure 3.7b.

➤ Closed-hT1R2

Sequences identity = 24.34 %

Sequences similarity = 39.75 %

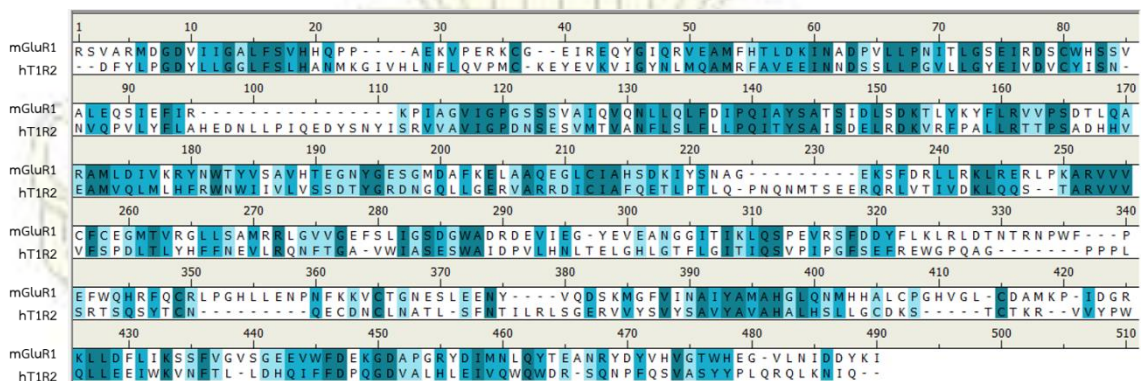


Figure 3.1 Sequence alignment between mGluR1 (closed-mT1R2) and hT1R2.

➤ Closed-hT1R3

Sequences identity = 22.35 %

Sequences similarity = 39.09 %

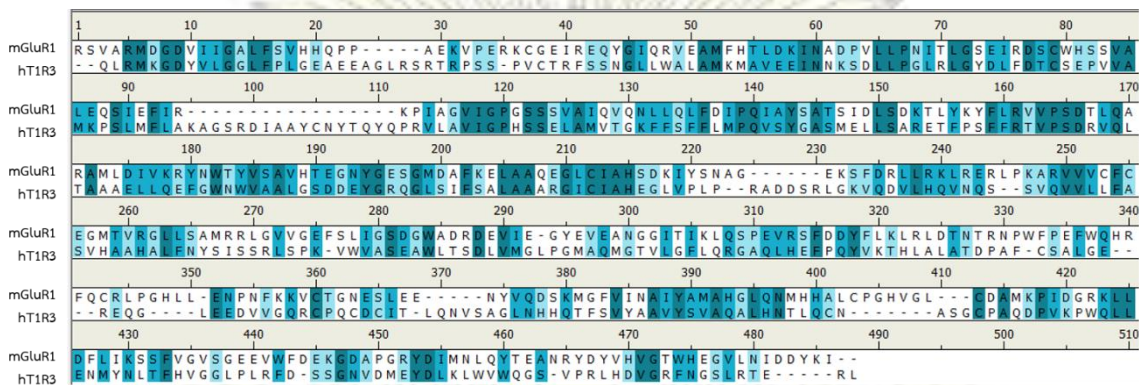


Figure 3.2 Sequence alignment between mGluR1 (closed-mT1R2) and hT1R3.

➤ Open-hT1R2

Sequences identity = 24.47 %

Sequences similarity = 39.88 %

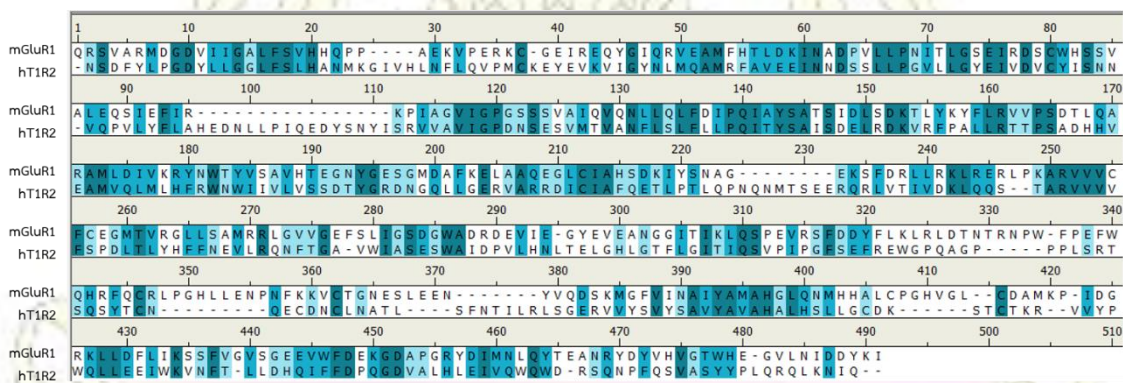


Figure 3.3 Sequence alignment between mGluR1 (open-mT1R3) and hT1R2.

➤ Open-hT1R3

Sequences identity = 22.01 %

Sequences similarity = 40.37 %

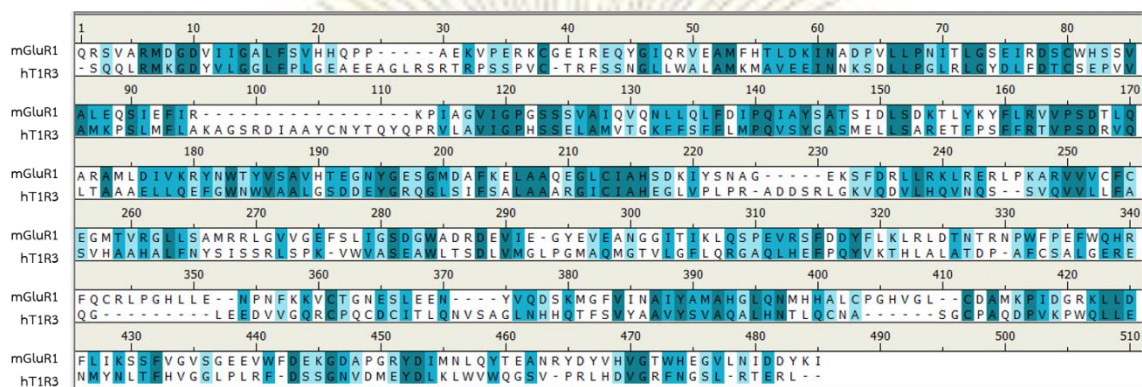


Figure 3.4 Sequence alignment between mGluR1 (open-mT1R3) and hT1R3.

(a) closed-hT1R2/open-hT1R3

(b) open-hT1R2/closed-hT1R3

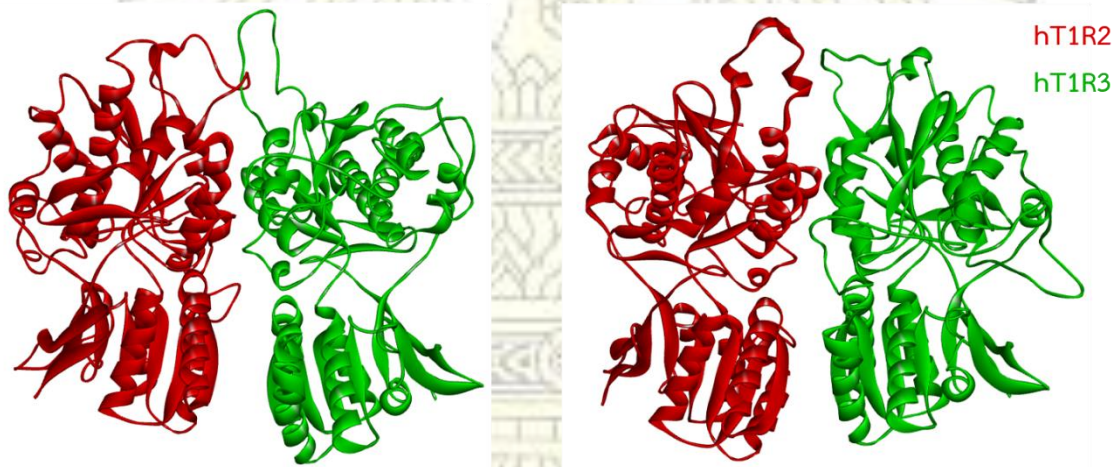


Figure 3.5 The models of human sweet taste receptor: (a) closed-hT1R2/open-hT1R3 and (b) open-hT1R2/closed-hT1R3.

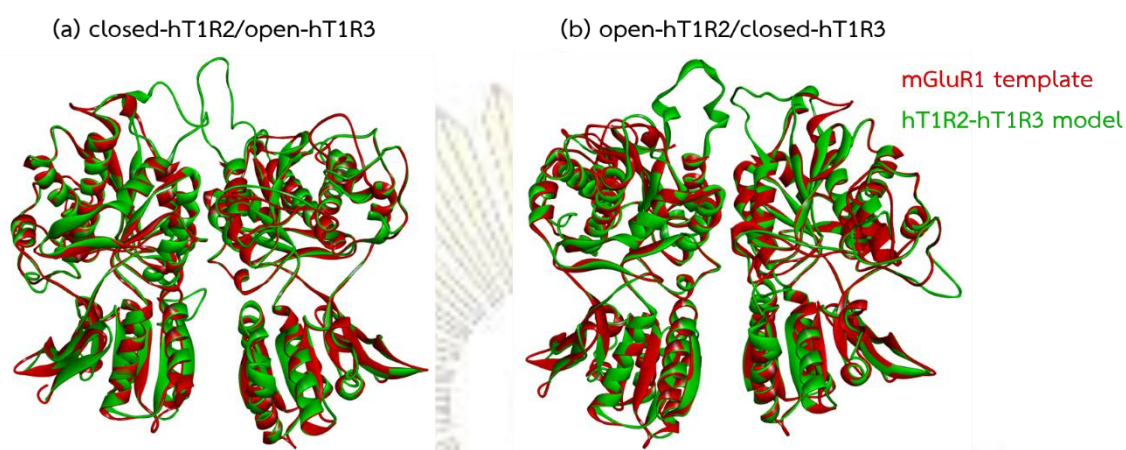


Figure 3.6 Superimposition between mGluR1 template and the models of human sweet taste receptor: (a) closed-hT1R2/open-hT1R3 and (b) open-hT1R2/closed-hT1R3.

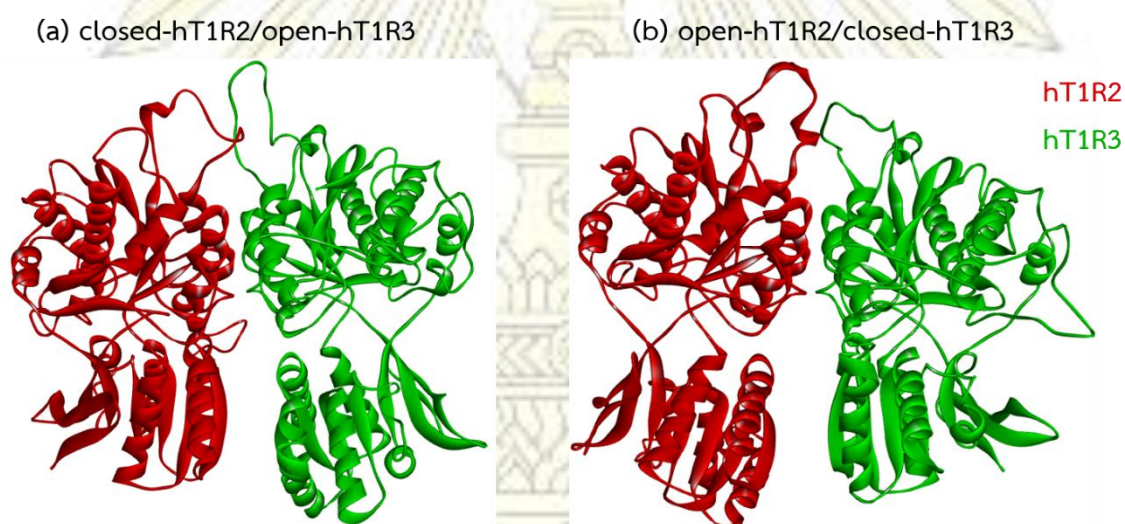


Figure 3.7 Homology models of human sweet taste receptor: (a) closed-hT1R2/open-hT1R3 and (b) open-hT1R2/closed-hT1R3.

3.2 Molecular docking simulation

ClusPro server was used for the docking study between hT1R2/hT1R3 and brazzein. Brazzein was blind docked into the 2 forms of hT1R2/hT1R3. Docking result showed that there were the 2 possible complexes of closed-hT1R2/open-hT1R3 with brazzein (Figure 3.8) and the 3 possible complexes of open-hT1R2/closed-hT1R3 with brazzein (Figure 3.9). The protein-protein interaction energies of the complexes were summarized and compared in Tables 3.1 and 3.2, respectively. These 5 models were selected for studying the complexes in aqueous solution by molecular dynamics simulation.

Table 3.1 The interaction energies (kcal/mol) between closed-hT1R2/open-hT1R3 and brazzein.

closed-hT1R2/open-hT1R3	Lowest Energy
complex 1	-826.8
complex 2	-851.1

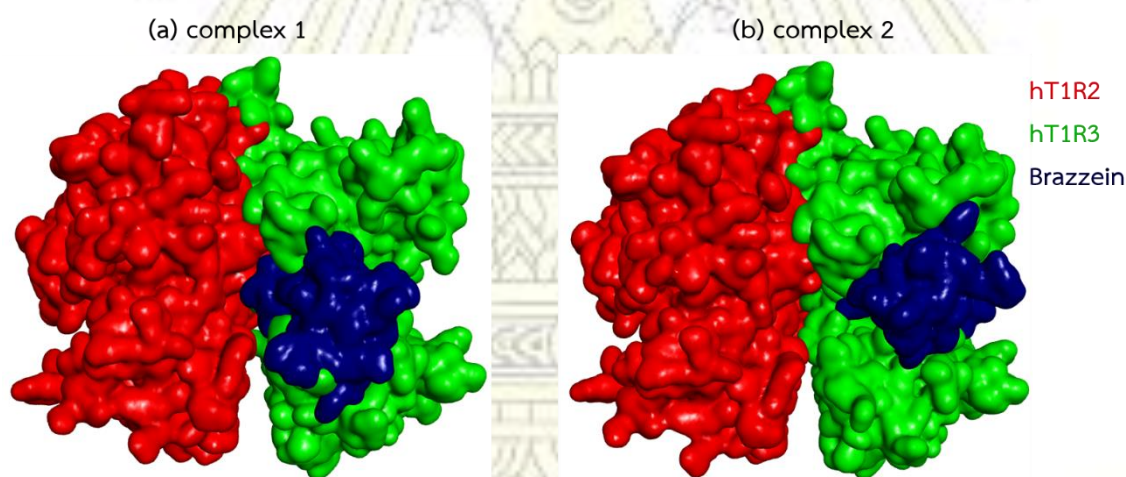
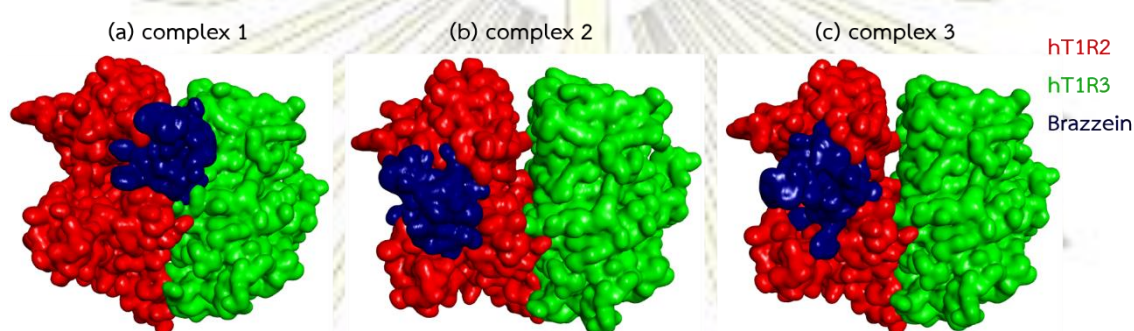


Figure 3.8 Two possible structures of closed-hT1R2/open-hT1R3 in complex with brazzein: (a) complex 1 and (b) complex 2.

Table 3.2 The interaction energies (kcal/mol) between open-hT1R2/closed-hT1R3 and brazzein.

open-hT1R2/closed-hT1R3	Lowest Energy (kcal/mol)
complex 1	-968.7
complex 2	-932.4
complex 3	-929.2

**Figure 3.9** Three possible structures of open-hT1R2/closed-hT1R3 with brazzein:

(a) complex 1, (b) complex 2 and (c) complex 3.

3.3 Molecular dynamics simulation

MD simulations of all systems were performed for 100 ns under periodic boundary condition using AMBER 16 program. The last snapshots of closed-hT1R2/open-hT1R3 and open-hT1R2/closed-hT1R3 were shown in Figures 3.10 and 3.11.

The cpptraj module was used to compute the structural analyses as follows. The equilibrium state of all simulated models was determined by computing the 1D- and 2D-root-mean-square displacements (1D-RMSD and 2D-RMSD). The b-factor and root-mean-square fluctuation (RMSF) calculations were used to investigate the fluctuation of the simulated protein structure. The protein-protein hydrogen bonds at the interface were calculated to observe the formation of hydrogen bonding throughout the simulation. Moreover, the MM/GBSA binding free energy calculations were performed to predict the preferential binding site, key binding amino acid residues involved in brazzein binding, and binding affinity of the complexes.

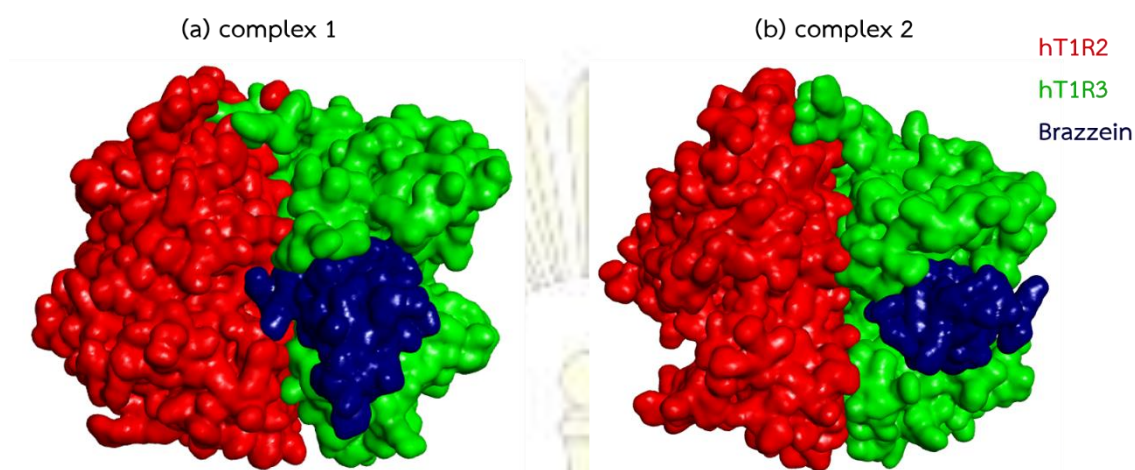


Figure 3.10 Last snapshot of closed-hT1R2/open-hT1R3 with Brazzein:
(a) complex 1 and (b) complex 2.

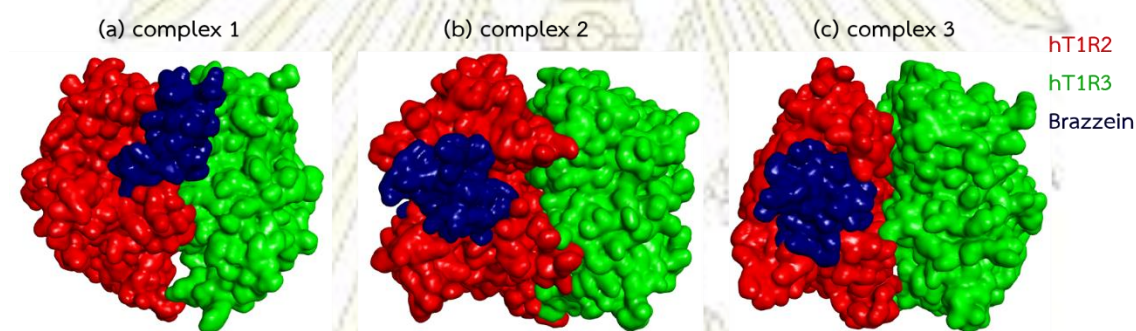


Figure 3.11 Last snapshot of open-hT1R2/closed-hT1R3 with Brazzein:
(a) complex 1, (b) complex 2 and (c) complex 3.

3.4 System stability

The stability of MD system was analyzed by the 1D- and 2D-root-mean-square displacement (RMSD) calculation. In Figure 3.12, the 1D-RMSD values of all atoms for a whole complex (red) as well as its hT1R2 (blue), hT1R3 (cyan) and brazzein (black) of all systems rapidly increase at the first 20 ns then the RMSD values of complex of (a) closed-hT1R2/open-hT1R3 receptor in apo form, (c) and (e) closed-hT1R2/open-hT1R3 and open-hT1R2/closed-hT1R3 receptors in brazzein bound forms fluctuated between 5 to 6 Å, (b) and (f) closed-hT1R2/open-hT1R3 and open-hT1R2/closed-hT1R3 receptor in brazzein bound forms fluctuated between 4.5 to 5.5 Å, (d) open-hT1R2/closed-hT1R3 receptor in apo form fluctuated between 6 to 7 Å and (g) open-hT1R2/closed-hT1R3 receptor in

brazzein bound forms fluctuated between 5.5 to 6.5 Å. All systems seem to reach the equilibrium state at ~80 ns. The 2D-RMSD results (Figure 3.13) suggest the stability of the system by the colors. All systems show cyan to blue colors at the last 20 ns correlated with the 1D-RMSD results. In this study, the last 20-ns MD trajectories of each system were extracted for further analysis in terms of structural dynamics, MM/GBSA binding free energy and decomposition free energy.

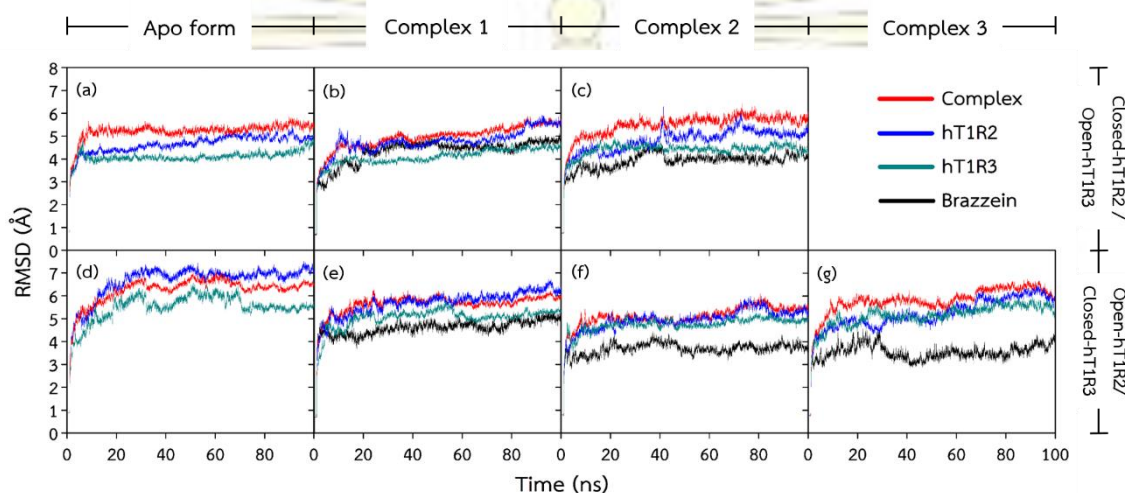


Figure 3.12 RMSD plots of all atoms for systems: (a) closed-hT1R2/open-hT1R3 receptor in apo form and (b-c) in brazzein bound forms, (d) open-hT1R2/closed-hT1R3 receptor in apo form and (e-g) in brazzein bound forms.

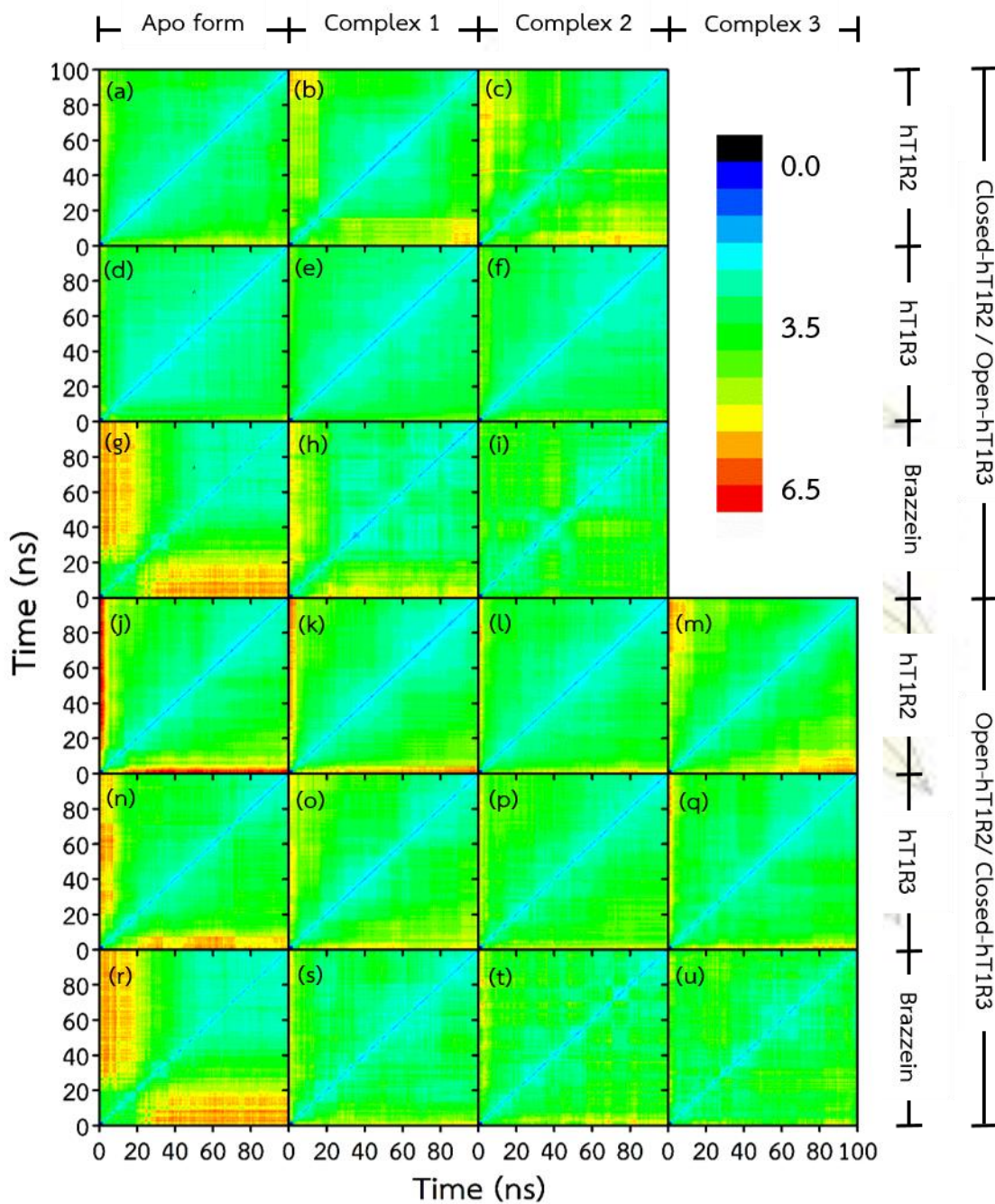


Figure 3.13 2D-RMSD plots of hT1R2, hT1R3 and brazzein for closed-hT1R2/open-hT1R3 and open-hT1R2/closed-hT1R3 in apo and brazzein bound forms.

3.5 Structural stability

The fluctuation of protein structure was analyzed by the b-factor and root-mean-square fluctuation (RMSF) calculations. In Figure 3.14, the complexation with brazzein in complex 2 (c) cause the lower RMSF values compared with its apo form (a) but the RMSF values of other complexes (b, e, f and g) are not different. B-factor gives the information of the structural stability by the colors of the protein. The rigid and flexible proteins are shaded in blue and red. The B-factor results show that when the brazzein binds with both forms of hT1R2/hT1R3 receptor, the protein structure at the binding site is more stable.

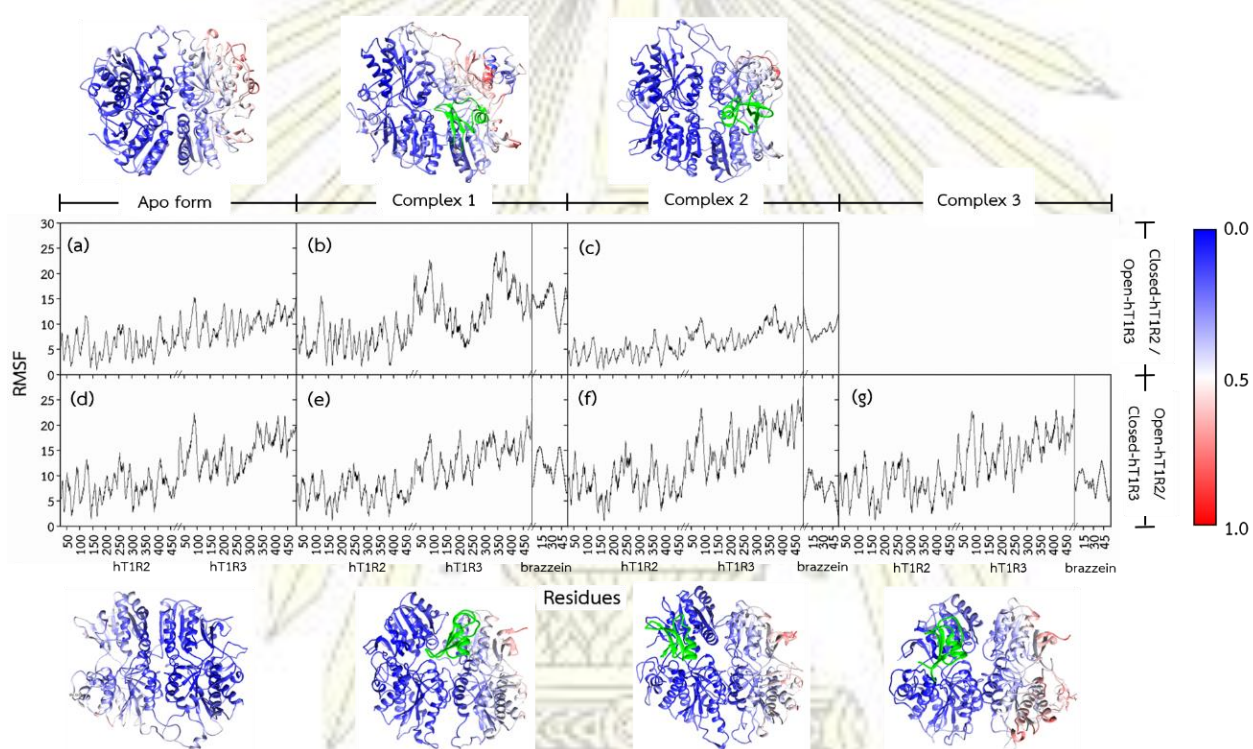


Figure 3.14 B-factor and RMSF values of all atoms for systems: (a) closed-hT1R2/open-hT1R3 receptor in apo form and (b-c) in brazzein bound forms, (d) open-hT1R2/closed-hT1R3 receptor in apo form and (e-g) in brazzein bound forms.

3.6 Binding affinity prediction

MM/GBSA method was used to investigate the binding free energy ($\Delta G_{\text{bind(MM/GBSA)}}$) of brazzein binding to the hT1R2/hT1R3 receptor. The results are given in Table 3.3 together with its energetic components, the gas phase energy (ΔE_{MM}) as a summation of ΔE_{vdW} and ΔE_{ele} energies, the solvation free energy (ΔG_{solv}) as a summation of ΔG_{nsolv} and ΔG_{psolv} energy. ΔE_{ele} contribution is stronger than ΔE_{vdW} in all simulations. In both closed-hT1R2/open-hT1R3 and open-hT1R2/closed-hT1R3, brazzein only binding to the open form of hT1R3 and hT1R2, respectively (more detail in Figure 3.15), which correlated with previous work [9]. In complex 2 is significantly more preferential with $\Delta G_{\text{bind(MM/GBSA)}}$ of -62.94 ± 0.87 kcal/mol and -61.30 ± 0.78 kcal/mol, respectively. Due to the limitation of entropy calculation, the $\Delta G_{\text{bind(MM/GBSA)}}$ of these two systems cannot be directly compared.

Table 3.3 The binding free energy (kcal/mol) of the complexes between closed-hT1R2/open-hT1R3, open-hT1R2/closed-hT1R3 in complex with brazzein.

	closed-hT1R2/open-hT1R3 in complex with brazzein		open-hT1R2/closed-hT1R3 in complex with brazzein		
	Complex 1	Complex 2	Complex 1	Complex 2	Complex 3
ΔE_{vdW}	-129.29 ± 0.70	-107.90 ± 0.78	-123.43 ± 0.70	-133.07 ± 0.90	-106.65 ± 0.82
ΔE_{ele}	-628.04 ± 5.56	-432.73 ± 5.72	-209.56 ± 3.35	-537.09 ± 3.59	-403.92 ± 6.50
ΔE_{MM}	-757.33 ± 5.72	-540.63 ± 5.51	-332.99 ± 3.36	-670.15 ± 3.78	-510.58 ± 6.92
ΔG_{nsolv}	-18.68 ± 0.07	-14.84 ± 0.09	-16.83 ± 0.09	-19.25 ± 0.11	-15.74 ± 0.14
ΔG_{psolv}	724.18 ± 5.09	492.53 ± 4.99	305.09 ± 3.13	628.10 ± 3.46	495.54 ± 6.07
ΔG_{solv}	705.50 ± 5.05	477.69 ± 4.99	288.26 ± 3.09	608.85 ± 3.40	479.80 ± 5.97
$\Delta G_{\text{bind(MM/GBSA)}}$	-51.83 ± 1.12	-62.94 ± 0.87	-44.72 ± 0.70	-61.30 ± 0.78	-30.77 ± 1.27

3.7 Contract residues for brazzein binding

On the basis of MM/GBSA approach, the per-residue decomposition free energy ($\Delta G_{\text{bind}}^{\text{residue}}$) and its energetic components, electrostatic (ΔE_{ele} and ΔG_{psolv}) and van der Waals (ΔE_{vdW} and ΔG_{nsolv}) terms, were calculated to identify the key amino acid residues for brazzein binding interaction. The total decomposition free energies of each amino acid residues ($\Delta G_{\text{bind}}^{\text{residue}}$) of hT1R2 and hT1R3 that bind with brazzein of all systems were shown in Figure 3.15, where the positive and negative decomposition free energy values represent the brazzein destabilization and stabilization, respectively. In case of brazzein binding with closed-hT1R2/open-hT1R3 in the complexes 1 and 2, there are 8 amino acid residues (E170, R176, R226 of hT1R2 and R52, L245, P246, R252, L308 of hT1R3) and 7 amino acid residues (F65, N68, D216, E217, H278, D307, L308 of hT1R3) that have $\Delta G_{\text{bind}}^{\text{residue}} \leq -2.0$ kcal/mol, respectively. In case of open-hT1R2/closed-hT1R3 binding with brazzein, there are both 12 amino acid residues in complex 1 (I50, V51, E63, L245, P247, N248, M251, L281 of hT1R2 and R191, A228, L229, A232 of hT1R3) and complex 2 (Y64, I69, Y284, H285, P310, V311, E317, N376, L381, S382, G383, E384 of hT1R2) that have $\Delta G_{\text{bind}}^{\text{residue}} \leq -2.0$ kcal/mol but in complex 3, there are only 5 amino acid residues (I50, Y64, Q249, Y284, V311 of hT1R2). The E170 (in hT1R2: complex 1) and D216, E217 (in hT1R3: complex 2) of brazzein binding with closed-hT1R2/open-hT1R3, were found to be the key binding residues for brazzein binding, in a correspondence with previous study [9], which used alanine-scanning mutagenesis to identify the key amino acid residues involved in binding interaction.

Moreover, the energy stabilization from the important residues ($\Delta G_{\text{bind}}^{\text{residue}} \leq 1.0$ kcal/mol) was separately considered in terms of the contribution from sidechain (red bar) and backbone (green bar) as well as the electrostatic (ΔE_{ele} and ΔG_{psolv} , black line) and vdW (ΔE_{vdW} and ΔG_{nsolv} , light grey line) energies of brazzein binding with closed-hT1R2/open-hT1R3 and open-hT1R2/closed-hT1R3 were shown in Figures 3.16 and 3.17, respectively. The results have shown that the binding energies of hT1R2/hT1R3 and brazzein mainly come from sidechain and vdW energies.



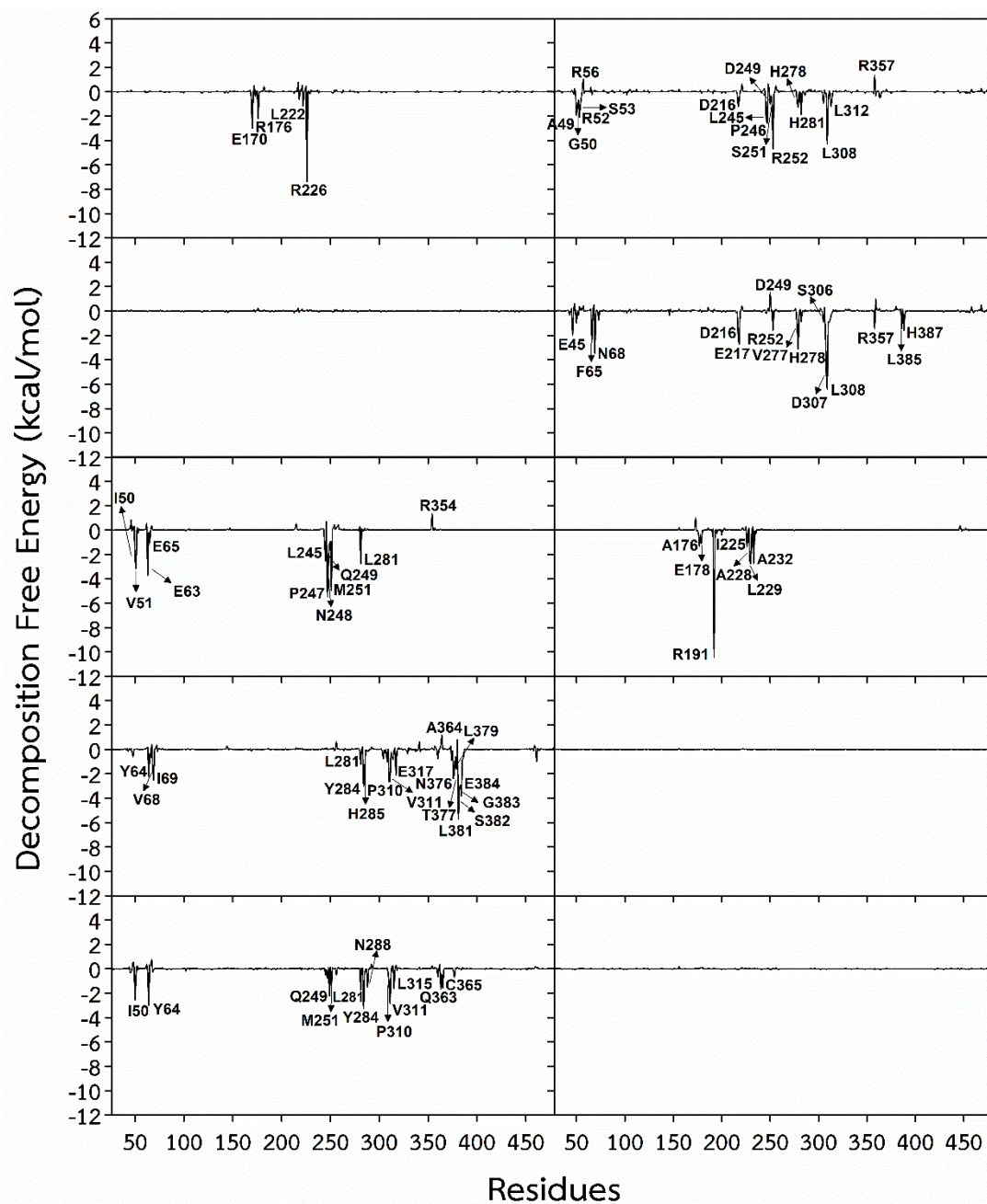


Figure 3.15 Per-residue decomposition free energy ($\Delta G_{\text{bind}}^{\text{residue}}$, kcal/mol) of hT1R2 (left) and hT1R3 (right) domains for brazzein binding with closed-hT1R2/open-hT1R3 (a-d) and open-hT1R2/closed-hT1R3 (e-j) based on MM/GBSA method.

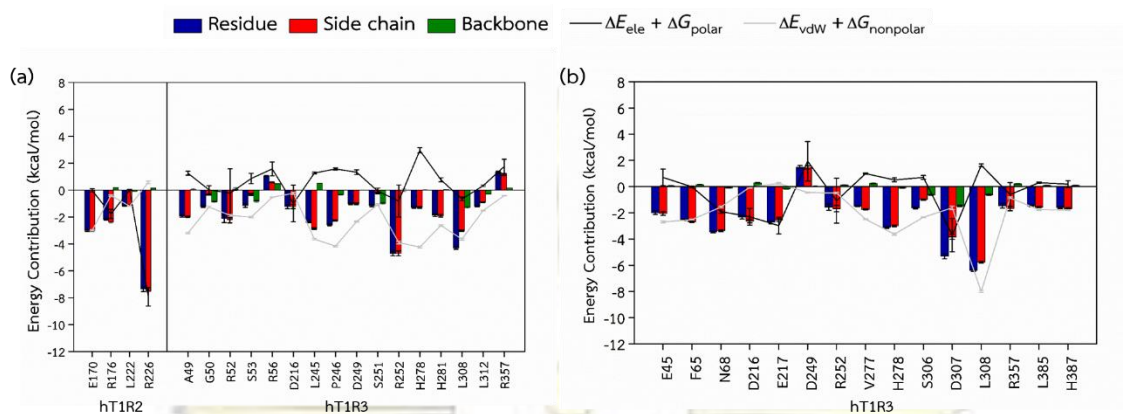


Figure 3.16 The decomposition free energy (kcal/mol) from the residue (blue bar), side chain (red bar) and backbone (green bar) of closed-hT1R2/open-hT1R3 receptor contributing to brazzein binding. The electrostatic ($\Delta E_{\text{ele}} + \Delta G_{\text{polar}}$) and vdW ($\Delta E_{\text{vdW}} + \Delta G_{\text{nonpolar}}$) energetic terms were represented by black and light grey lines, respectively.

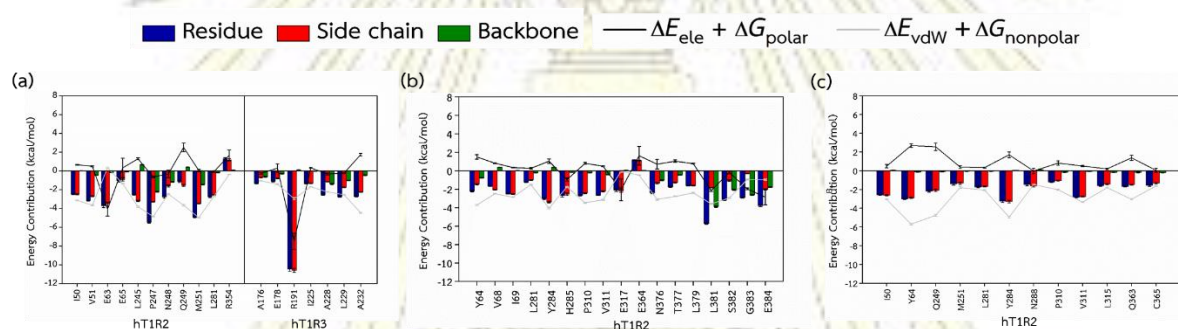


Figure 3.17 The decomposition free energy (kcal/mol) from the residue (blue bar), side chain (red bar) and backbone (green bar) of open-hT1R2/closed-hT1R3 receptor contributing to brazzein binding. The electrostatic ($\Delta E_{\text{ele}} + \Delta G_{\text{polar}}$) and vdW ($\Delta E_{\text{vdW}} + \Delta G_{\text{nonpolar}}$) energetic terms were represented by black and light grey lines, respectively.

3.8 Hydrogen bonding interaction

The number of H-bond formed between hT1R2/hT1R3 and brazzein along the simulation were plotted in Figure 3.18. Brazzein binding with closed-hT1R2/open-hT1R3 in complex 2 (Figure 3.18b) has 20-40 H-bonds with hT1R3 domain, while the number of h-bonds with both domains in complex 1 (Figure 3.18a) were somewhat missing during the last 30 ns of simulation. In the case of open-hT1R2/closed-hT1R3, brazzein interacts with both domains in complex 1 (Figure 3.18c) but only with hT1R2 in complexes 2 and 3 (Figures 3.18d and 3.18e, respectively). The complex 2 has the number of H-bond (25-50) importantly higher than complex 3 (20-40).

Moreover, the number of H-bond between hT1R2 and hT1R3 were compared when the hT1R2/hT1R3 binding and not binding with brazzein (Figure 3.19). The results show that when brazzein bind with closed-hT1R2/open-hT1R3 as complex 2 (Figure 3.19c) lead to higher number of H-bond than the closed-hT1R2/open-hT1R3 without brazzein (Figure 3.19a). In another way, brazzein bind with open-hT1R2/closed-hT1R3 as complex 2 (Figure 3.19f) cause the lower number of H-bond than open-hT1R2/closed-hT1R3 didn't bind to the brazzein (Figure 3.19d). So, brazzein prefer to bind the closed-hT1R2/open-hT1R3 more than open-hT1R2/closed-hT1R3.

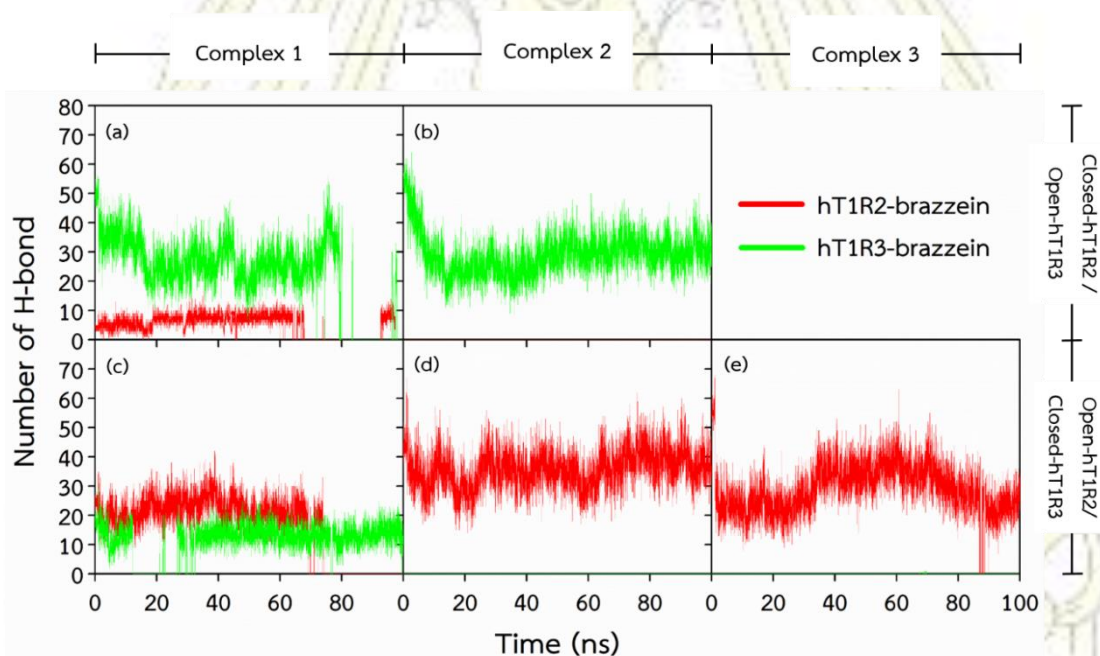


Figure 3.18 The number of H-bond between hT1R2 and brazzein, hT1R3 and brazzein for brazzein binding with closed-hT1R2/open-hT1R3 (a-b) and open-hT1R2/closed-hT1R3 (c-e).

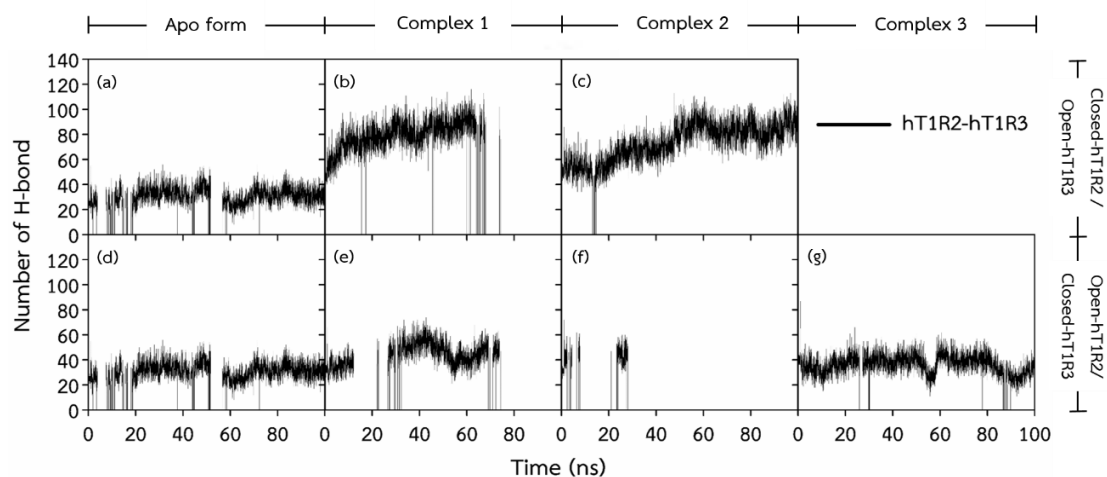


Figure 3.19 The number of H-bond between hT1R2 and hT1R3 for (a) closed-hT1R2/open-hT1R3 in apo form, (b-c) brazzein binding with closed-hT1R2/open-hT1R3, (d) open-hT1R2/closed-hT1R3 in apo form and (e-f) brazzein binding with open-hT1R2/closed-hT1R3.



Chapter 4

Conclusion

The molecular modelling approaches were used to investigate the structural insights into complexes between two forms of human sweet taste receptor (closed-hT1R2/open-hT1R3 and open-hT1R2/closed-hT1R3) and the sweet-taste protein (brazzein). The 1D- and 2D-RMSD results revealed that all systems reached the equilibrium at ~80 ns and the last 20 ns MD trajectories of each model were subsequently extracted for further analysis. The results showed that the sweet-taste protein, brazzein, prefer to bind with the human sweet taste receptor which is open subunit. The MM/GBSA binding free energy, per-residue decomposition energy and number of H-bond results have shown that human sweet taste receptor (hT1R2-hT1R3), which hT1R2 is in the closed form and hT1R3 is in the open form, is the active conformation to bind with brazzein. Moreover, brazzein bind with closed-hT1R2/open-hT1R3 as complex 2 is the most possible structure.



References

- [1] Walters, D.; Hellekant, G. Interactions of the Sweet Protein Brazzein with the Sweet Taste Receptor. *J Agric Food Chem.* **2006**, 54(26), 10129-10133.
- [2] Lipman, D.; Pearson, W. Rapid and sensitive protein similarity searches. *Science* **1985**, 227, 1435-1441.
- [3] Berman, H.; Westbrook, J.; Feng, Z.; Gilliland, G.; Bhat, T.; Weissig, H.; Shindyalov, I.; Bourne, P. The Protein Data Bank. *Nucl. Acids Res* **2000**, 28, 235-242.
- [4] Finn, R.; Mistry, J.; Schuster-Bocker, B.; Griffiths-Jones, S.; Hollich, V.; Lassmann, T.; Moxon, S.; Marshall, M.; Khanna, A.; Durbin, R.; Eddy, S.; Sonnhammer, E.; Bateman, A. Pfam: clans, web tools and services. *Nucl. Acids Res* **2006**, 34, 247-251.
- [5] How does our sense of taste work? PubMed Health [Online], August 17, 2016, <https://www.ncbi.nlm.nih.gov/pubmedhealth/PMH0072592/>
- [6] Janssen, S. Depoortere | Nutrient sensing in the gut: new roads to therapeutics? *Trends Endocrinol Metab.* **2013**, 24(2), 92-100. doi: 10.1016/j.tem.2012.11.006.
- [7] Laffitte, A.; Neiers, F.; Briand, L. Functional roles of the sweet taste receptor in oral and extraoral tissues. *Curr Opin Clin Nutr Metab Care.* **2014**, 17(4), 379–385.
- [8] Pin, J.; Kniazeff, J.; Goudet, C.; Bessis, A.; Liu, J.; Galvez, T.; Acher, F.; Rondard, P.; Prézeau, L. The activation mechanism of class-C G-protein coupled receptors. *Biol Cell* **2004**, 96, 335–342.
- [9] Assadi-Porter, F. M.; Maillet, E. L.; Radek, J. T.; Quijada, J.; Markley, J. L.; Max, M. Key Amino Acid Residues Involved in Multi-Point Binding Interactions between Brazzein, a Sweet Protein, and the T1R2–T1R3 Human Sweet Receptor. *Journal of Molecular Biology* **2010**, 398(4), 584-599.
- [10] Ming, D.; Hellekant, G. Brazzein, a new high-potency thermostable sweet protein from *Pentadiplandra brazzeana* B. *FEBS Lett.* **1994**, 355(1), 106-108.
- [11] Izawa, H.; Ota, M.; Kohmura, M.; Ariyoshi, Y. Synthesis and characterization of the sweet protein brazzein. *Biopolymers* **1996**, 39, 95–101.
- [12] Caldwell, J. E.; Abildgaard, F.; Dzakula, Z.; Ming, D.; Hellekant, G.; Markley, J. L. Solution structure of the thermostable sweet-tasting protein brazzein. *Nat. Struct. Biol.* **1998**, 5(6): 427–431.

- [13] Johnson, M.; Srinivasan, N.; Sowdhamini, R.; Blundell, T. Knowledge-based protein modeling. *Crit Rev Biochem Mol Biol.* **1994**, 29(1), 1-68.
- [14] França, T. Homology modeling: an important tool for the drug discovery. *J Biomol Struct Dyn.* **2015**, 33(8), 1780-93. doi: 10.1080/07391102.2014.971429.
- [15] Zhexin, X. Advances in Homology Protein Structure Modeling. *Curr Protein Pept Sci.* **2006**, 7(3), 217-227.
- [16] Sanchez, R.; Sali, A. Comparative protein structure modeling as an optimization problem. *J. Mol. Struct. (Theochem)* **1997**, 398-399, 489-496.
- [17] Xuan-Yu, M.; Hong-Xing, Z.; Mihaly, M.; Meng, C. Molecular Docking: A powerful approach for structure-based drug discovery. *Curr Comput Aided Drug Des.* **2011**, 7(2), 146-157.
- [18] Fischer, E. Einfluss der configuration auf die wirkung derenzyme. *Ber. Dt. Chem. Ges.* **1894**, 27, 2985-2993.
- [19] Molecular Docking Service. *Creative Proteomics* [online]. <https://www.creative-proteomics.com/services/molecular-docking-service.htm>
- [20] Vajda, S.; Yueh, C.; Beglov, D.; Bohnuud, T.; Mottarella, S. E.; Xia, B.; Hall, D. R.; Kozakov, D. New Additions to the ClusPro Server Motivated by CAPRI. *Proteins* **2017**, 85(3), 435-444.
- [21] Kozakov, D.; Brenke, R.; Comeau, S.R.; Vajda, S. PIPER: an FFT-based protein docking program with pairwise potentials. *Proteins* **2006**, 65, 392-406.
- [22] Chuang, G.; Kozakov, D.; Brenke, R.; Comeau, S. R.; Vajda, S. DARS (Decoys As the Reference State) Potentials for Protein-Protein Docking. *Biophys J.* **2008**, 95(9), 4217-4227.
- [23] Norbert, A.; Kurt, B.; Helmut, G.; Kurt, K. Introduction to Molecular Dynamics Simulation. *John von Neumann Institute for Computing* **2004**, 23, 1-28.
- [24] Genheden, S.; Ryde, U. The MM/PBSA and MM/GBSA methods to estimate ligand-binding affinities. *Expert Opinion on Drug Discovery* **2015**, 10(5), 449-461.
- [25] Kollman, P. A.; Massova, I.; Reyes, C.; Kuhn, B.; Huo, S.; Chong, L.; Lee, M.; Lee, T.; Duan, Y.; Wang, W.; Donini, O.; Cieplak, P.; Srinivasan, J.; Case, D. A.; Cheatham T. E. Calculating structures and free energies of complex molecules: combining molecular mechanics and continuum models. *Acc Chem Res* **2000**, 33(12), 889-897.

Curriculum Vitae

Miss Nutsarun Wangsawangrun was born on June 21, 1996 in Bangkok, Thailand. In 2013, she graduated from Sirirattanathorn School, Bangkok, Thailand. In 2014, she was admitted to a Bachelor's degree program: major in Chemistry, Faculty of Science, Chulalongkorn University and would complete the program in 2018. Her address is 54, Udomsuk 52 Lane, Sukhumvit 103 Road, Bangna Sub-district, Bangna District, Bangkok 10260. Her email address is june_1100@hotmail.com.

